

Analyzing Impact of DER on FIDVR - Comparison of EMT Simulation of a Combined Transmission and Distribution Grid with Aggregated Positive Sequence Models*

Deepak Ramasubramanian¹, Parag Mitra, Papiya Dattaray, Mobolaji Bello, Jens C. Boemer, Anish Gaikwad

Grid Operations & Planning Group, Electric Power Research Institute, Knoxville, Tennessee, USA

Abstract

The increase in percentage of distributed energy resources (DERs) brings in a degree of uncertainty in bulk power system planning and operations. Further, the presence of $1-\phi$ induction motors introduces the possibility of motor stalling and fault induced delayed voltage recovery (FIDVR). With newer versions of IEEE Std 1547TM there can be the opportunity to obtain dynamic voltage support from DERs. In this paper, the impact of DERs providing dynamic voltage on the dynamic behavior of $1-\phi$ induction motors is examined in detail along with an exploration of the need for simulation platforms that go beyond positive sequence. The studies discussed here are carried out both in detailed electromagnetic time domain and in positive sequence domain for comparison.

Keywords: Co-simulation, dynamic voltage support, fault induced delayed voltage recovery

1. Introduction

The increase in percentage of distributed energy resources (DER) brings in a degree of uncertainty in bulk power system planning and operations. Additionally, it also introduces an element of uncertainty with regard to distribution planning and operations, especially with regard to the dynamic behavior of DERs in juxtaposition with the behavior of induction motors. Traditionally, the bulk power system has provided short circuit strength and stiffness to the distribution system, which enables induction motors to start and successfully ride through faults. However with an increase in DERs causing the retirement of bulk power system connected generation, an added concern is the availability of adequate system strength at the transmission and distribution interface.

*This work was supported in part by U.S. Department of Energy under Award Number DE-EE0009019

¹dramasubramanian@epri.com

Legacy interconnection standards such as IEEE Std 1547TM-2003 [1] allowed for DERs to trip from the distribution system very rapidly upon the occurrence of a voltage or frequency event. In most cases, DERs were allowed to almost instantaneously trip if their terminal voltage fell below 0.88pu. Such an operation practice was primarily driven by distribution operation and safety practices at the time wherein DERs were still relatively low in percentage and thus, distribution operations preferred to have a passive distribution network while responding to system events. However, as the percentage of DER increases, this restrictive operation model could result in further issues to be resolved during system events. Additionally, the large loss of active power (due to trip of DERs), especially when the system requires it the most, could cause cascading impacts on the power system.

For example let us assume that the percentage of DERs in a load center (e.g. a major city) is 75% of the load [2]. This results in a 25% loading of the surrounding transmission and sub-transmission network. Upon the occurrence of a transmission system single line to ground fault (statistically has the highest probability of occurrence), due to a common substation distribution transformer winding configuration with a Δ winding on the transmission side and a Y configuration on the distribution side, two phases on the distribution side would experience a low voltage (around 0.58pu for a solid fault on the primary side)[3, 4]. Assuming an equal distribution of $1 - \phi$ DERs across the three phases, this single line to ground fault could result in 66% of $1 - \phi$ DERs ceasing to energize and tripping almost instantaneously on the distribution system. Further, all $3 - \phi$ DERs would also trip due to activation of a trip command based on least phase voltage. The total loss of active power supplied by DERs could now be almost 75% of the total DER output. Note here that although IEEE Std 1547TM-2003 did not explicitly specify an instantaneous trip for voltages below 0.88pu, neither did it explicitly specify a duration of time for which the DERs must remain energized and connected to the network. The wording in the standard was open to interpretation as it stated that the DERs shall trip *within* 2.0s. Combining this wording with the state of the art distribution operation and safety practice that was prevalent at the time, a conservative assumption is that of an instantaneous trip. Due to this, the loading on the surrounding transmission and sub-transmission system could increase to 50%. As a result of DER tripping, the voltage on the distribution system could fall which can result in increased stalling of induction motors. This sudden increase in transmission system loading could also further increase the voltage drop. As this reduction in voltage (and its associated impact) occurs within a short-term time frame [5], the voltage drop cannot be mitigated by conventional distribution voltage regulation equipment such as load tap changers or regulators that typically have longer response times. Additionally, because of the change in spinning reserve allocation due to retirement of the conventional generation to accommodate the increase in DER, loss of active power from DER could result in an impact on the frequency response of the system, unless this loss is accounted for when performing reserve procurement, which would come at a cost to the consumer. All these factors could cumulatively result in a cascading loss of load service thereby impacting system reliability metrics.

Recognizing this, recent updates on the IEEE Std 1547TM (IEEE Std 1547aTM-2014, IEEE Std 1547TM-2018, and IEEE Std 1547aTM-2020) [6, 7, 8] have continuously introduced requirements for wider voltage and frequency ride-through capabilities and trip settings for additional smart inverter functionalities such as dynamic voltage support. However presently, the threshold values and timers related to the trip settings have a range of applicability, while the degree to which the capability of the smart inverter functionalities is used is left to the decision of the respective electric utilities in whose footprint the DER interconnects. Further, due to the nature of the interconnection process and the continuous evolution of the standard, although a more recent standard may be available, unless the electric utility requires the use of the recent standard (as detailed out in the corresponding interconnection requirements) there can be an added uncertainty from the perspective of the planner/operator, regarding which standard is being followed for legacy and newly interconnecting DERs.

As the behavior of increased percentage of DER has an impact on the bulk power transmission system, technical interconnection requirements for DERs should have input from transmission planning and operation engineers [9]. Major points that need to be addressed in the technical interconnection requirements relate to:

1. Value of voltage thresholds at which the DER enters momentary cessation,
2. Value of voltage thresholds at which the DER's trip timers activate,
3. Value of the time at which the DER would trip after activation of the trip timers,
4. Requirement for activation of smart features such as dynamic voltage support and/or frequency support, and
5. Priority order (whether active or reactive) used for current injection.

Note here that although information related to requirements (2) and (3) above are beneficial and important, they are not specifically denoted in the IEEE 1547 standards. The IEEE 1547 standards only specify trip clearing times. Here, the focus is predominantly on inverter based DER although parameters related to trip and voltage support would equally apply to non-synchronous DER. Traditionally, despite the presence of induction motor loads, distribution networks were classified as passive networks. This resulted in distribution networks being represented as static loads in transmission planning analysis. However, the low voltage caused by transmission faults can potentially induce $1 - \phi$ induction motors to stall and if not tripped, can delay the recovery of voltage upon clearance of the fault. This phenomena has been termed as fault induced delayed voltage recovery (FIDVR).

FIDVR is a phenomenon where the system voltages take a significantly long time to recover to the pre-fault levels following a fault [10]. It is typically caused by the stalling of the compressor motors of single-phase residential air-conditioners (residential HVAC) during a fault [11, 12]. In a locked rotor condition, these motors draw significantly large amounts of both active and reactive power resulting in depressed voltages for an extended period. The voltages slowly recover as the stalled single-phase compressor motors are tripped by their thermal protection systems. Low voltages during FIDVR can result in load loss [13] and in some extreme cases could possibly lead to large scale

voltage collapse. A secondary effect of large amount of load loss are over voltages, which can damage power system components. Therefore, accurately modeling FIDVR for system studies is crucial. In bulk power system stability studies, the use of the composite load model allows for an approximate aggregated representation of residential HVACs that can cause FIDVR following a fault [14, 15].

Mitigation of FIDVR, by utilizing a system level approach, predominantly takes the form of additional dynamic reactive support [15] whose value and location can be determined by framing and solving a variety of optimization problems [16, 17, 18]. With the rapid deployment of power electronic devices, the use of static var compensators (SVC) connected to the transmission network at critical locations is used in many power systems to help mitigate FIDVR [19, 20, 21, 22]. These devices are connected at the transmission level as it is practically and not economically viable to install many small voltage compensators in the distribution network. However with increase in DERs, their smart inverter capabilities [23] can be leveraged to provide mitigation options for FIDVR events [24, 25, 26]. Recent work [27] has also attempted to derive a quantitative estimation of the effectiveness of using DER to mitigate FIDVR. These articles in literature, and many such more, attempt to address the objective of mitigating FIDVR through development of improved control techniques. However, there are very few articles that address the topic of comparing the benefit derived from different categories and operation modes of DER. Our paper addresses this topic as it has implication on planning of the power system.

An increasingly active distribution network with the presence of a variety of smart inverter control methods along with interactions with induction motors also raises the question of accuracy of the existing state of the art composite load models for use in bulk power system planning studies. Additionally, there is a need to ascertain whether simulation tools that go beyond positive sequence [28] simulation environments are required from a bulk power system planning perspective.

In this paper, the impact of DER on the stalling and recovery of single phase induction motor loads will be documented. The entire transmission system and the distribution system will be represented in detail in an electromagnetic simulation platform. The paper will aim to assess the ability of DER to mitigate the stalling of induction motor loads, and the settings of DER that provide most benefit. Additionally, it would also aim to identify scenarios that would need the use of detailed representation of the distribution system for bulk power planning studies. In this paper, co-simulation is considered to be the combined simulation of both transmission and distribution network with both networks represented in detail within the same simulation software. Reference [28] provides an overview of co-simulation platforms for transmission planning.

2. System studied and representation of DER and motor load

A modified New England 39 bus system [29] was used to represent the transmission network. In addition to reducing the size of the network, the impedance of few transmission paths was increased in order to enable creation of a load pocket following

clearance of a fault. The load pocket results in a depressed transmission voltage when the low impedance path is opened with the fault. The impedance of the branches and transformers in the network is tabulated in Table 1. All static load were represented as constant current for active power and constant impedance for reactive power. To represent a distribution network, a feeder as shown in Fig. 1 was connected at buses 3, 4, and 18 on the transmission network. This feeder is representative of a distribution feeder in Hawaii and has previously been used to study the impact of DER on stalling of induction motors [30, 31, 32]. In this prior study, the transmission system was however represented as a single equivalent source and thus, the impact of DERs were observed only within the local feeder. However, depending on the control settings of the DER, it was observed that DERs may have the capability to mitigate stalling of $1 - \phi$ induction motors.

The addition of DER to these feeders was arbitrarily done as one of the aims of this study was to ascertain the need of representing the transmission network to a level of detail greater than just an equivalent source. DERs were added only to the feeders connected to bus 3 and bus 4 and were not added to the feeder at bus 18 in order to observe whether the impact of DERs from the adjacent feeders will be perceived. Each DER was controlled to inject a constant value of active power (i.e. power reference which is independent of system frequency and voltage), within current limits, while having the capability to provide dynamic voltage support during abnormal voltage conditions and allow for adjustable momentary cessation voltage thresholds. Tripping of the DER was not considered. The controller of each DER was modeled along the lines of the inverters controls described in [33].

Within the feeder, single phase residential HVAC systems were modeled using the model developed previously in [34, 35]. Each $1 - \phi$ induction motor in the feeder is a combination of numerous 5.278 kW motors. The load torque on the motor has speed dependent torque component of 6 $N.m$ super imposed with a sawtooth torque component with an average value of 8 $N.m$, which is characteristic of a reciprocating compressor load torque. An approximate speed based relay to mimic thermal overload tripping is represented. Further, there is a small degree to imbalance in the total loading of the feeder across the three phases.

3. Analysis in Electromagnetic Transient Domain

As transmission and distribution systems were both modeled in the same simulation platform (all simulations were conducted in an electromagnetic transient (EMT) simulation environment) to the same level of detail, a possible realistic future transmission system scenario was considered with inverter based resources (IBR) representing all generation sources. Although the rating of each individual IBR generation source is around 800 - 1200 MW, it can be considered to be large wind farms or HVDC connections. Thus, the entire transmission network is now essentially a zero inertia network (or 100% IBR network). All IBRs are also modeled along the lines of the inverter controls specified in [33] and shown in Fig. 2. This control structure has been shown in

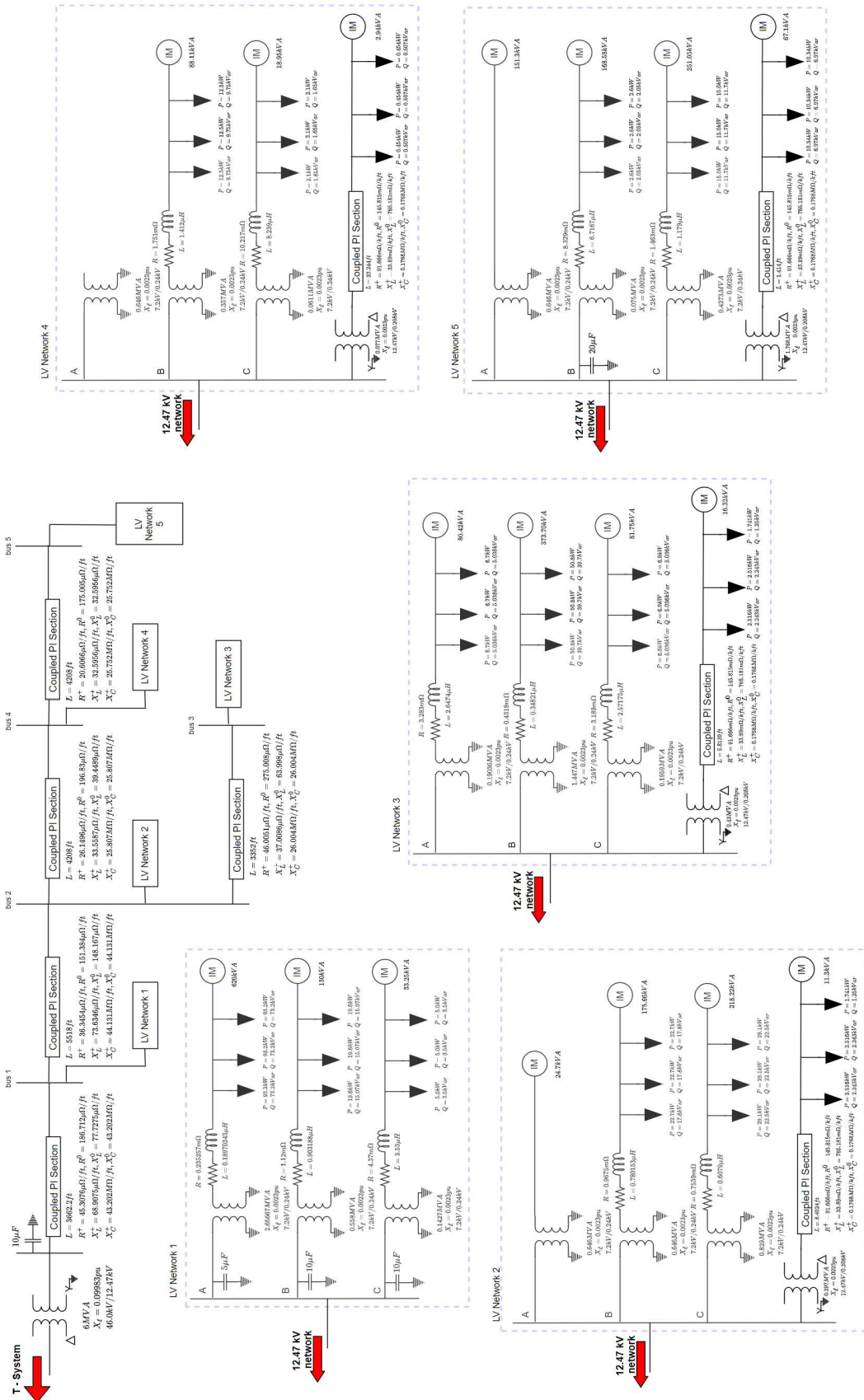


Figure 1: One line diagram of distribution feeder connected at transmission network buses 3, 4, and 5

Table 1: Impedance of branches and transformers in the transmission network

From bus	To bus	R (pu)	X (pu)	B (pu)
1	2	0.0035	0.0411	0.6987
1	39	0.0010	0.0250	0.75
2	3	0.0013	0.2151	0.2572
2	25	0.0070	0.0086	0.1460
3	4	0.0013	0.1213	0.2214
3	18	0.0011	0.0133	0.2138
4	5	0.0008	0.2128	0.1342
4	14	0.0008	0.2129	0.1382
5	6	0.0002	0.0026	0.0434
5	8	0.0008	0.0112	0.1476
6	7	0.0006	0.0092	0.1130
6	11	0.0007	0.0082	0.1389
7	8	0.0004	0.0046	0.0780
8	9	0.0023	0.0363	0.3804
9	39	0.0010	0.0250	1.200
10	11	0.0004	0.0043	0.0729
10	13	0.0004	0.0043	0.0729
13	14	0.0009	0.0101	0.1723
14	15	0.0018	0.0217	0.3660
15	16	0.0009	0.0094	0.1710
16	17	0.0007	0.0089	0.1342
17	18	0.0007	0.2082	0.1319
17	27	0.0013	0.0173	0.3216
25	26	0.0032	0.0323	0.5130
26	27	0.0014	0.0147	0.2396

From bus	To bus	X (pu)	MVA base
2	30	0.0181	100.0
3	feeder	0.08	36.0
4	feeder	0.08	36.0
6	31	0.0250	100.0
10	32	0.020	100.0
11	12	0.0435	100.0
12	13	0.0435	100.0
18	feeder	0.08	36.0
25	37	0.0232	100.0

[33] to allow for stable operation of a 100% inverter system. All transmission system IBRs were in reactive current priority mode with a maximum current of 1.1pu. They also had automatic voltage control enabled.

To observe the impact of various operational features of DER on induction motors, a variety of DER scenarios were studied as tabulated in Table 2. All DER were also assumed to be reactive current priority mode. Additionally, all DERs were 3 – ϕ and connected at 12.47kV buses within the feeder. For the feeder connected to Bus 3 of the transmission network, DERs were placed at buses 2, 4, and 5 of the feeder while for the feeder connected to Bus 4 of the transmission network, DERs were placed at buses 2 and 3 of the feeder. In each case, an 80ms fault was applied on the line between bus 2 and bus 3 of the transmission network, at a distance of 0.1% from bus 3. Upon clearing the fault, the line between bus 2 and bus 3 was opened 10ms later. Two alternate post contingency system topology were considered, one with creation of a load pocket (load area which is deficient in reactive power support) around bus 3 and bus 18 and one without the creation of the load pocket.

3.1. Without DER

Before observing the impact of DER, the dynamic response of the system without any DER is ascertained. For the 3 – ϕ fault with clearance of the line, Fig. 3 shows the response observed at the T&D interface of all three feeders. Upon clearance of the fault and the corresponding line, a load pocket is created with bus 3 and bus 18. The large and sustained increase in reactive power consumption (in comparison to the pre-fault loading level) is characterized by the stalling of 1 – ϕ induction motors who eventually trip 2s later. Trip of the stalled motors is noted by the reduction in the active and reactive power consumption measured at the substation head or the T&D interface and

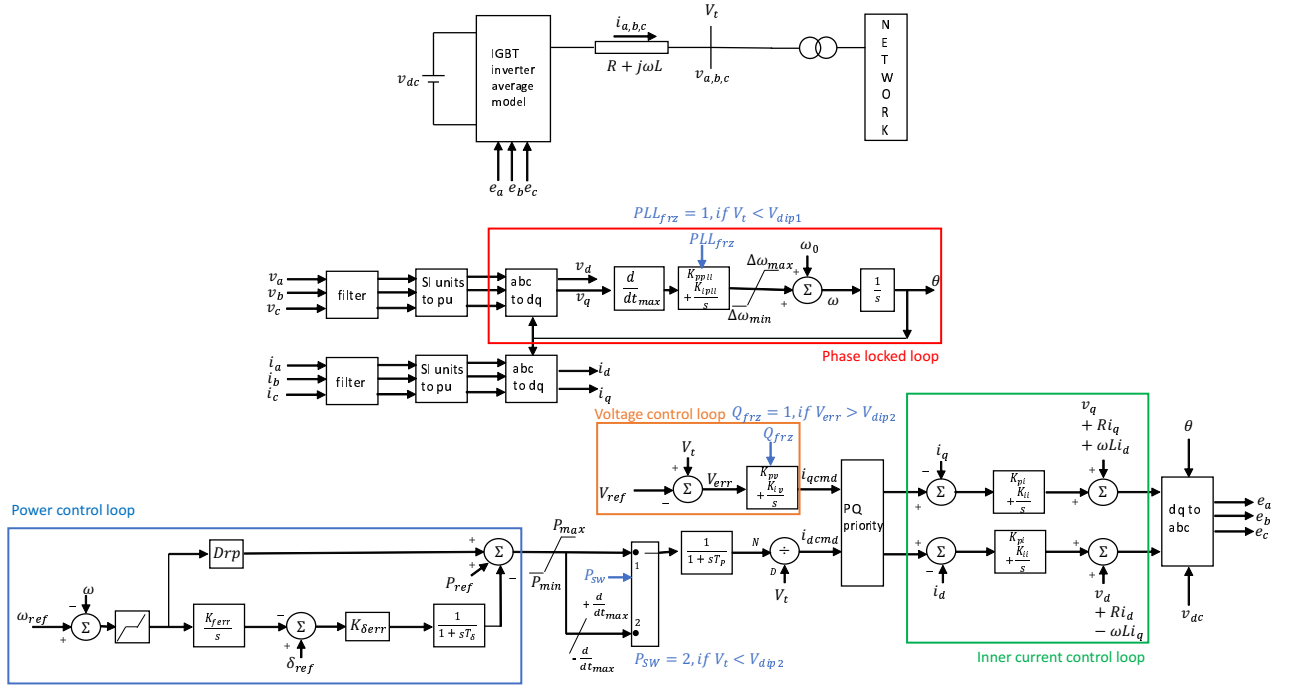


Figure 2: Block diagram of control architecture used for both transmission connected and distribution connected inverter sources

also by the reduction in active consumption. However, due to the formation of the load pocket, the voltages remain at a value of approximately 0.8pu. Additionally, the feeders at bus 3 and bus 18 are impacted to an equal and larger extent when compared to the feeder at bus 4. As a result of feeders at bus 3 and bus 4 being equally impacted, their voltage plots are superimposed over each other. Of the fourteen $1 - \phi$ induction motors on each feeder, on the feeders at bus 3 and bus 18 only one $1 - \phi$ induction motor was able to successfully ride through the fault on each feeder. On the feeder at bus 4, eleven (11) out of the fourteen motors were able to successfully ride through the fault. The speed of the $1 - \phi$ induction motors on each feeder is shown in Fig. 4.

The $1 - \phi$ induction motors in our study trip based on a speed vs. time threshold. Even after tripping the motors, the voltage remains depressed due to the creation of a load pocket on the transmission network as a result of opening line between buses 2 and 3. The opening of this line creates a higher impedance path in the region which subsequently results in a lower voltage. In order for the voltage to recover, more load may have to be tripped at the adjoining buses. However, at these buses since the feeder is not represented in detail and rather load is represented as an aggregate load, a under voltage based tripping scheme has not been implemented as such a scheme cannot be implemented arbitrarily. Implementation on load shedding schemes are a planning exercise on their own. Thus, since the low voltage persists even without adding DER, it is taken as a baseline for comparison to observe the impact of DER.

Further, with all transmission energy sources being IBRs, one could possibly assume that the absence of any voltage sources (like synchronous machines) is the cause of

Table 2: DER scenarios studied

Case	DERs	MVA of each DER	V_{MC} (pu)	DVS	DVS deadband (pu)	K_p DVS	K_i DVS	Comments	Scenarios
0	OFF								LLL-G fault with creation of load pocket LL fault with creation of load pocket L-G fault with creation of load pocket L-G delayed cleared fault with creation of load pocket LLL-G fault without creation of load pocket LL fault without creation of load pocket L-G fault without creation of load pocket L-G delayed cleared fault without creation of load pocket
1	ON	3	0.88	OFF					LLL-G fault with creation of load pocket
2	ON	3	0.50	OFF					LLL-G fault with creation of load pocket
3	ON	3	0.50	ON	0.0	0.1	10.0		LLL-G fault with creation of load pocket
4	ON	3	0.50	ON	0.1	5.0	0.0		LLL-G fault with creation of load pocket
5	ON	3	0.50	ON	0.1	10.0	0.0		LLL-G fault with creation of load pocket
6	ON	6	0.50	ON	0.1	5.0	0.0		LLL-G fault with creation of load pocket
7	ON	6	0.50	ON	0.1	10.0	0.0		LLL-G fault with creation of load pocket
8	ON	6	0.50	OFF					LLL-G fault with creation of load pocket
9	ON	3	0.50	ON	0.1	5.0	0.0	Additional DER on feeder head	LLL-G fault with creation of load pocket LL fault with creation of load pocket L-G fault with creation of load pocket L-G delayed cleared fault with creation of load pocket LLL-G fault without creation of load pocket LL fault without creation of load pocket L-G fault without creation of load pocket L-G delayed cleared fault without creation of load pocket

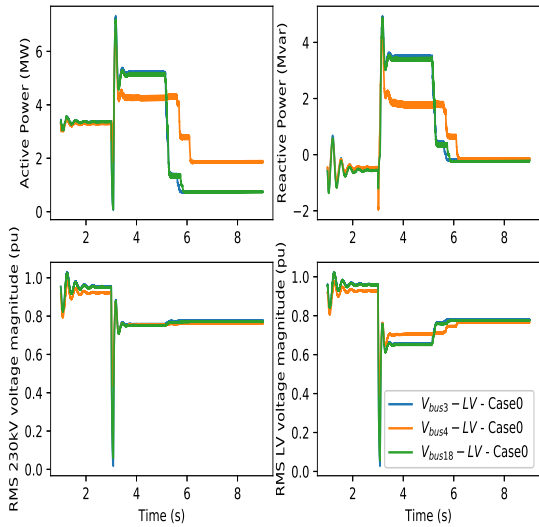


Figure 3: Without any DER, active power, reactive power and voltage magnitude at the T&D interface

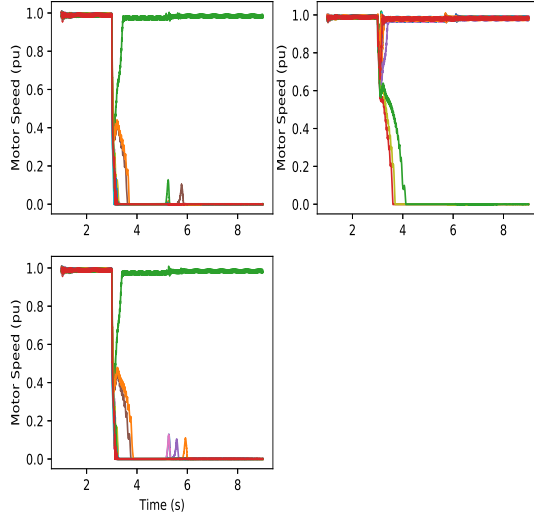


Figure 4: Without any DER, speed of fourteen $1-\phi$ induction motors of all three feeders (Feeder 3 top left, feeder 4 top right, feeder 18 bottom left)

stalling of the $1-\phi$ induction motors. To verify this, all IBRs were replaced with ideal voltage sources (source impedance approximately equal to 0.0) with a similar power flow solution. The fault current and the magnitude of voltage observed at bus 3 is shown in Figs. 5 and 6 respectively. It can be seen that with either ideal voltage source or IBRs, the fault current and voltage observed at bus 3 have the same trend. Thus, with all transmission sources being IBRs, in this particular study, there is negligible reduction in short circuit strength as observed from the location of the feeders. However, if the sources were of lower ratings, then there can be a possibility of a difference in behavior as discussed in [36, 37].

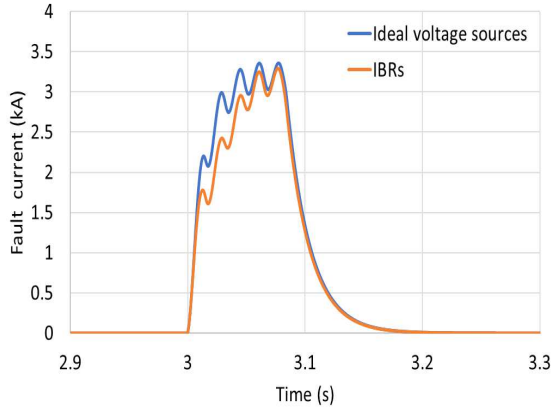


Figure 5: With the load pocket, comparison of fault current between the sources being ideal voltage sources and IBRs

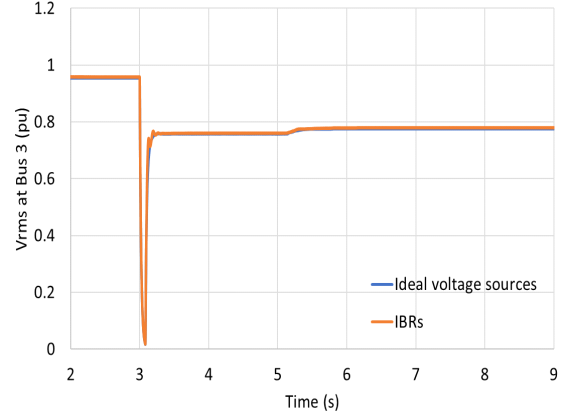


Figure 6: With the load pocket, comparison of voltage magnitude as bus 3 between the sources being ideal voltage sources and IBRs

Given that the base behavior of the network without DERs shows the stalling and trip of $1 - \phi$ induction motors, with the addition of DERs the aim would be to assess the DER control options that might help all induction motors successfully ride through the faults. Here, successful fault ride through indicates that following clearance of the fault, a $1 - \phi$ induction motor would be able to re-accelerate and reach close to steady state operation speed following clearance of the fault.

3.2. DER without dynamic voltage support

On feeder at bus 3, to start, 3 DERs of 3 MVA each (total 9 MVA) were placed on the feeder while on the feeder at bus 4, only 2 DERs of 3 MVA each (total 6 MVA) were placed. At both these locations, the ratio of DER to load is greater than 100% as the total gross load on the feeder is approximately 3 MW. However, initially each DER was assumed to be a legacy DER following IEEE Std 1547TM-2003. Due to this, the DERs had a momentary cessation voltage threshold of 0.88pu without any reactive power support functionality. To represent momentary cessation, when the voltage goes below the defined threshold, the current reference commands of the control loop are immediately set to 0.0 in order to cease to inject current. However, the inverter does not disconnect from the network. It still remains electrically connected to the network, just operating at 0.0 current. Once the voltage recovers, the current references are restored. The dynamic response of the network with this configuration of DERs is shown in Fig. 7. The presence of the DERs on the feeders at bus 3 and bus 4 is seen from the plot of active power at the T&D interface with reverse active power flow into the transmission network from the distribution network. However, because of the 0.88pu momentary cessation threshold, upon occurrence of the fault and subsequent clearance of the line, not only do induction motors stall and subsequently trip as before, the DERs do not inject any current as the voltage stays below 0.88pu. Due to this, the DERs have no beneficial impact on the behavior of the network. Rather, the permanent blocking of the DERs increases the loading on the transmission network following the clearance of the line.

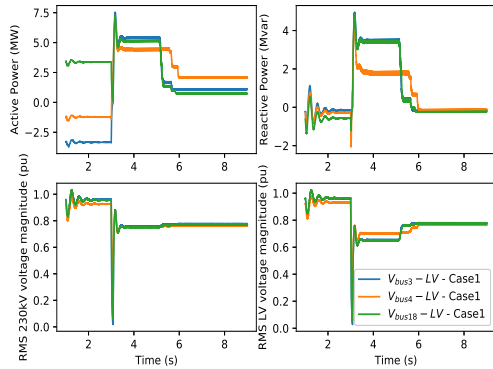


Figure 7: Active power, reactive power and voltage magnitude at the T&D interface of all three feeders with legacy DER

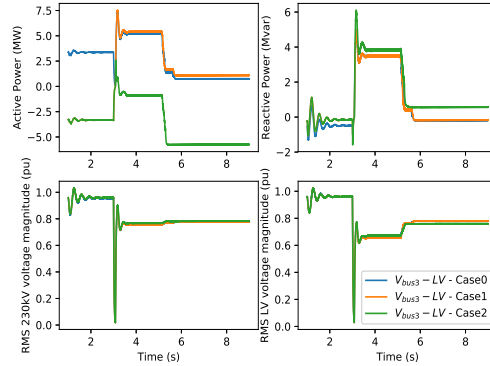


Figure 8: Active power, reactive power and voltage magnitude at the T&D interface of bus 3 comparing the response with reduction in momentary cessation voltage threshold

Additionally, many grid codes may have specifications regarding a ramp rate limit on recovery of active current following a low voltage disturbance. In this work we have not considered an explicit scenario to observe a comparison of response with low ramp rates. However, with a lower ramp rate, there will be more reactive power support provided to single phase induction motors from the distribution connected inverters while active power support would be provided by the inverter sources in the transmission network. This may result in more motors being able to ride through the event. Since one of the objectives of this paper is to compare the response between EMT and phasor models, a higher ramp rate is considered as it would result in a more stressed scenario which makes it more ideal for model comparison purposes.

As the major impact on the system is at bus 3, all subsequent results will be primarily shown for the feeder at bus 3. The first mitigation mechanism that can be implemented is reduction of the momentary cessation threshold from 0.88pu to 0.50pu. The response is as shown in Fig. 8. In this scenario, reduction of the momentary cessation threshold did not improve the voltage response of the system, nor did it have a substantial beneficial impact on the stalling and recovery of all induction motors. However, during the fault, lower amount of DER goes into momentary cessation which could have a beneficial impact on post fault system frequency. Upon clearance of the fault as observed by the reduction of the active power flowing into the distribution feeder from the transmission network, the DERs come out of momentary cessation. However, as the DERs are not providing any form of voltage/reactive power support (observed in the reactive power flow across the T&D interface), the impact on induction motor behavior remains approximately the same as before. In this case on the feeder at bus 3, two more $1 - \phi$ induction motors were able to successfully ride through the fault, while three additional $1 - \phi$ motors were able to ride through on the feeder at bus 4. With this, all $1 - \phi$ induction motors on the feeder at bus 4 were able to successfully ride through the event. The impact on the feeder at bus 18 remained unchanged. Once the motors trip, there is an increase in active power flow from the distribution network to

the transmission network. Thus, if the 3- ϕ DERs only inject active power, lowering of the momentary cessation threshold by itself may not have a beneficial impact on the stalling of 1- ϕ induction motors.

This result however raises the question about conceptually allowing for voltage magnitude to be influenced through control of active power output of DERs. In a transmission network, due to the large value of X/R ratio of the transmission lines, active power and voltage magnitude are very weakly coupled. However, in a lower voltage distribution network, due to the smaller value of X/R ratio, a stronger coupling exists between active power and voltage magnitude. Given the existence of this coupling between active power and voltage magnitude, the reason behind the ineffectiveness of just reducing the momentary cessation threshold to allow for continued active power injection is to be explored. It is likely that as the 3- ϕ DERs are placed at the 12.47kV level and not on the secondary network, there is still weak coupling between active power and voltage magnitude as observed from the terminals of the DER. If 1- ϕ DERs were placed on the secondary network, a lower momentary cessation threshold without any reactive power support could have resulted in an improvement in voltage magnitude and a corresponding beneficial impact on 1- ϕ induction motors.

3.3. DER with dynamic voltage support

The next set of scenarios to be studied is the operation mode of DER providing dynamic voltage support (DVS). Although case 3 in Table 2 is the first scenario where DVS is enabled, the dynamic response associated with this case will be discussed later in this section as the controller structure used to obtain this DVS response is not on a pure proportional controller, but with the use of a proportional+integral control. Thus, the response and system behavior from provision of DVS through a proportional control (represented by the characteristic shown in Fig. 9) is shown in Figs. 10 and 11 for the feeder at bus 3.

With DERs providing reactive power support, the reactive power drawn by the feeder from the transmission network is lower. However, as each DER is a current limited device, providing reactive power support can be at the expense of active power injection. Here it can be seen with reactive power injection from DERs, the active power drawn by the feeder from the transmission network is greater when compared to the active power flow in case 2. Additionally, with DVS, there is a distinct improvement in the voltage response on the 12.47 kV network. This results in an additional 1- ϕ induction motor being able to successfully ride through the event on both the feeder at bus 3 and bus 18. Now, a total of four (4) 1- ϕ induction motors at bus 3, all fourteen (14) 1- ϕ induction motors at bus 4, and two (2) 1- ϕ induction

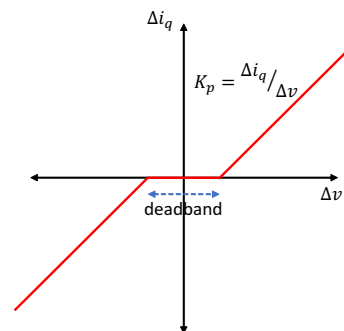


Figure 9: Characteristic representation of dynamic voltage support through proportional control

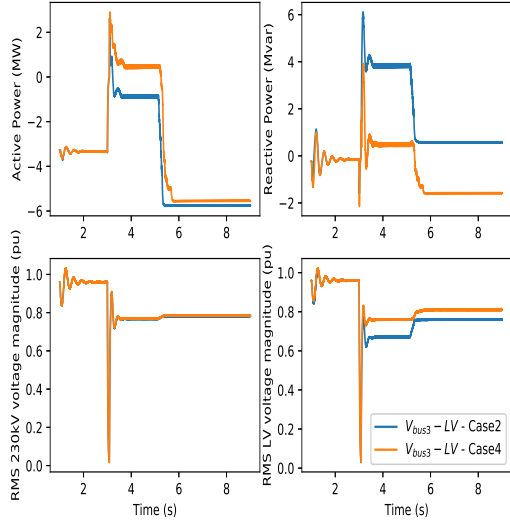


Figure 10: For Case 4, active power, reactive power and voltage magnitude at the T&D interface of bus 3 comparing the response with provision of DVS of different gains

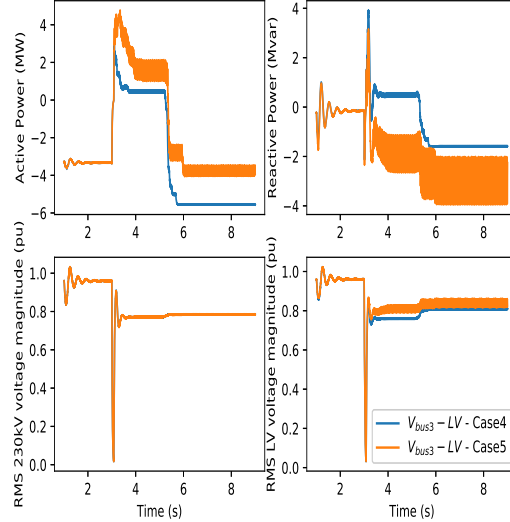


Figure 11: For Case 5, active power, reactive power and voltage magnitude at the T&D interface of bus 3 comparing the response with provision of DVS of different gains

motors at bus 18 successfully ride through the event. Although there is a distinct improvement in the voltage magnitude on the 12.47kV system, there is only a marginal improvement in the voltage in the upstream 230kV transmission system.

Is this minimal impact on the 230kV network due to the lower amount of reactive power support provided by the DVS? The feeder at bus 3 has 3 DERs each with a rating of 3 MVA. Thus, a total of 9 MVA capacity should ideally be available for reactive power (because of Q-priority). However, from Fig. 10 it can be seen that only around 4 Mvar of reactive power support is provided by the DERs. In case 4, DVS is obtained through a dead band of 0.1pu on the input voltage deviation, with a proportional gain of 5.0. Thus, if the entire 1.0pu current is to be obtained through DVS, the input voltage deviation would have to be 0.3pu. From the figure on the left it can be seen that 12.47kV voltage during the induction motor stalled state is around 0.8pu with DVS. For this voltage deviation, only 0.5pu reactive current (or 1.5 Mvar per each DER) is injected into the network.

Thus if additional reactive power is required through a proportional DVS, one option can be to make the control more aggressive by increasing the gain of the proportional controller. Since a gain of 5.0 resulted in a reactive current of 0.5pu, one option for increased control effort is to make the gain 10.0. Keeping all other parameters the same as in case 4, Fig. 11 shows the system dynamic response from case 5. The response is compared against the response obtained from case 4.

As a result of increasing the proportional control gain, the DVS control of the DERs within the feeder fight with each other as the injection of current from one DER causes a change in the voltage deviation at the terminals of the other DERs which results in a oscillatory response. In a radial system, such as the distribution feeder, it is not

advisable to have aggressive voltage controllers that aim to control the voltage along a sequential path of the radial connection. Since the voltage at various points in the network are dependent on the current flowing in the network, and since the value of current is itself dependent on the voltage levels, aggressive voltage control along the network can lead to numerical non-convergence of the interdependency. As a result, the aggressive voltage controllers of the various DER fight with each other. However, there is an increase in total reactive power support from the DERs as approximately an average of 3 Mvar of reactive power is injected into the transmission network. There is again a distinct difference in the 12.47kV voltage magnitude. A total of nine (9) $1 - \phi$ induction motors at bus 3 are now able to successfully ride through the fault. However, at bus 18, there is no improvement in induction motor behavior.

Another point to note is that the control interactions between DERs on the feeder at bus 3 remain within the distribution network as the 230kV transmission voltage does not show the oscillations. Further evidence of these control interactions remaining within the distribution system for this scenario can be seen in Fig. 12 from the response observed at the feeder connected on bus 18. It can be seen that the response is almost identical for case 4 and case 5. One reason for the localization of control interactions could be the presence of the effective high impedance path between bus 3 and bus 18 due to opening the line between bus 2 and bus 3 following clearance of the fault. If the two buses were strongly connected to each other, then there is a chance that the control interactions from the feeder at bus 3 could propagate to the other feeders.

Although case 5 shows the occurrence of control oscillations, it also provides an insight into the required level of reactive power support that may allow some/-many motors to re-accelerate back to their steady state operating speeds thereby reducing the severity of FIDVR. With this in mind, case 6 is set up with the DVS gain to be the same as case 4, but the rating of each DER is doubled to 6 MVA. Theoretically, this scenario should now provide the required level of reactive power while also maintaining controller stability. The response at bus 3 is show in Fig. 13. It can be seen that in comparison to case 4, in case 5 an additional reactive support of approximately 2 Mvar is provided. While this does not manifest in a large improvement in the voltage profile at the 12.47kV level, now a total of eleven (11) $1 - \phi$ induction motors at bus 3 are able to successfully ride through the fault. Further, on bus 18, an additional $1 - \phi$ induction motor successfully recovers bringing the total to 3 motors at bus 18.

Making the DVS control loop aggressive in this scenario (i.e. case 7 with a proportional gain of 10.0) resulted in a similar control interaction as observed in case 5.

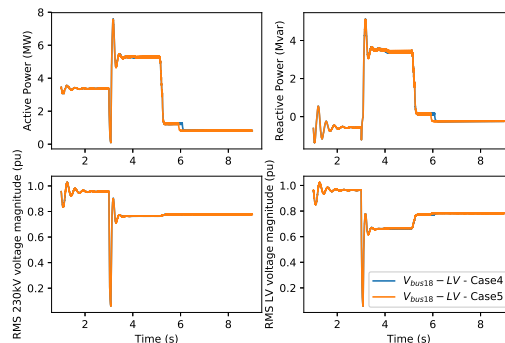


Figure 12: Active power, reactive power and voltage magnitude at the T&D interface of bus 18 comparing the response between two values of DVS proportional gain

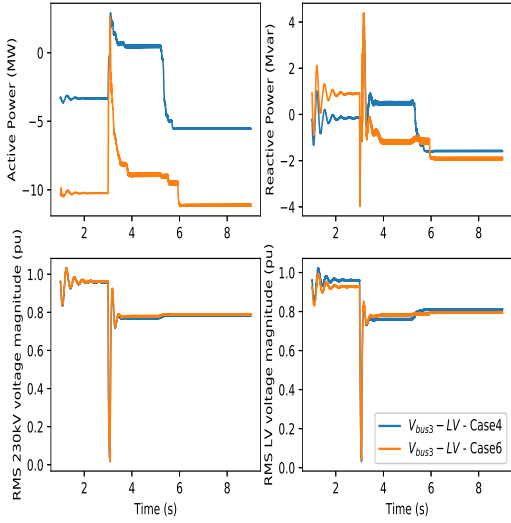


Figure 13: Active power, reactive power and voltage magnitude at the T&D interface of bus 3 comparing the response between two ratings of DER

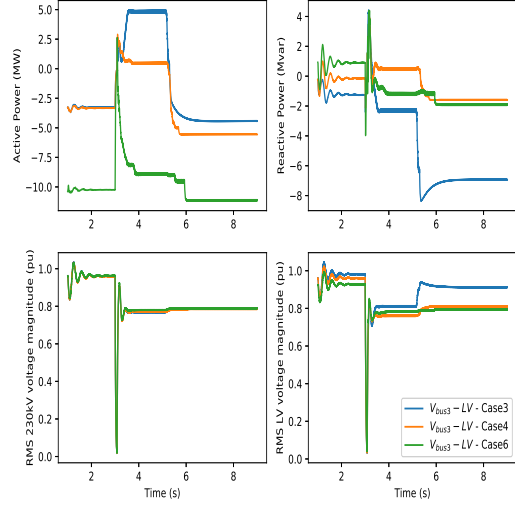


Figure 14: Active power, reactive power and voltage magnitude at the T&D interface of bus 3 comparing the response with DVS obtained through a 0.0pu dead band with integral control

However, despite the marginal stability of the system, all fourteen (14) $1 - \phi$ induction motors at bus 3 were able to successfully ride through the fault. Case 8 had a response similar to case 2. Due to this similarity, the plots of the response for these cases are not shown in this section.

In all the above scenarios, DVS was obtained with a dead band of 0.1pu and the magnitude of reactive current was proportional to the voltage error. A value of 0.1pu was chosen for the dead band as it falls near the boundary of the continuous operating region of specified in IEEE Std 1547TM. As a bookend scenario, it is worth taking a look at the response of the network if the dead band was 0.0pu (essentially allowing for provision of DVS as soon as the voltage deviates from the reference). Additionally, an integral gain of 10.0 was used to allow for the controller to aim to minimize the steady state error in voltage. Although this form of voltage control is common on transmission connected inverter based resources, it is usually not advisable to have an integral controller and a zero dead band on DERs as there is a greater probability of controller interactions/instability with multiple DERs along a radial distribution feeder aiming to minimize the steady state error in voltage at their respective terminals. The response of the system as observed at bus 3 for this case is shown in Fig. 14.

In this case, the DER controllers did not fight with each other and a distinct difference in the voltage response within the 12.47kV network is observable. However, although the reactive power support provided is greater than case 4 or case 6, it does not result in a significant difference in the number of $1 - \phi$ induction motors that were able to successfully ride through the fault. Only three (3) motors at bus 3 and two (2) motors at bus 18 were able to successfully ride through. This results in a voltage rise upon trip of the rest of the motors which also manifests as an increase in reactive power

injection into the transmission network due to the action of the integral controller. The voltage rise is also due to additional reactive power support from the integral action of the voltage controller. It must be recognized here that though this particular set of control gains did not provide a beneficial response, it is possible that with a larger value of K_p for DVS and a 0.0pu dead band, a more suitable response could be obtained. However implications of using of a 0.0pu dead band for voltage control within a radial feeder must be carefully studied before recommendation for implementation.

From the above analysis, it can be inferred that while additional reactive power support is beneficial for successful ride through of $1 - \phi$ induction motors, the delivery of this reactive power should be in a controlled manner to avoid control interactions between DERs. Further, the rating of the DER should also be considered. The feeder draws an active power load of approximately 3.5 MW. However, upon occurrence of the fault with subsequent opening of the line, in order to obtain a successful ride through, approximately 6 Mvar of reactive power is required. While increasing the rating of DERs from 3 MVA to 6 MVA (resulting in a total of 18 MVA of DER on a feeder with 3.5 MW of load) does help more $1 - \phi$ induction motors to ride through successfully, such a scenario could either be perceived as an extreme future scenario or a scenario where DER peak output does not coincide with load peak output.

3.4. Increase in number of DERs

Rather than increasing the rating of each DER on the feeder, in case 9 an additional $3 - \phi$ 3 MVA DER was added at the head of the feeder on the 12.47 kV network. Thus, the total rating of DERs at bus 3 now amounted to 12 MVA. The operational mode of all four DERs were however kept the same as in case 4 (refer to Table 2). The observed response of the system to the fault is shown in Figs. 15 and 16. It can be seen that the reactive power injection immediately after the fault is similar to that obtained from case 6 which had 18 MVA of DER. Further, compared to case 4 wherein only four (4) $1 - \phi$ induction motors successfully rode through the fault at bus 3, now ten (10) of the fourteen $1 - \phi$ induction motors were able to ride through the fault.

For the 14 $1 - \phi$ induction motors that were present in each feeder, a summary of the number of motors that were able to successfully ride through the fault for all scenarios studied is tabulated in Table 3. From all these scenarios an inference can be drawn that the provision of DVS from DERs can help some or many single phase induction motors to re-accelerate provided a sufficient amount of reactive support is delivered in a controlled manner. Further, the benefit obtained from DVS within a feeder does not seem to transfer further up into the transmission system to adjoining feeders. However, from this study, this inference only holds to $3 - \phi$ DERs connected along the primary trunk link of the feeder. The impact of any form of voltage support from DERs (either $3 - \phi$ or $1 - \phi$) connected on the secondary laterals of the feeder cannot be inferred. This will be a topic of future work.

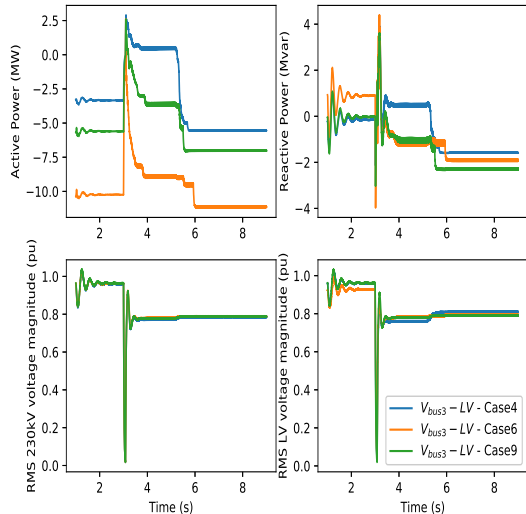


Figure 15: Active power, reactive power and voltage magnitude at the T&D interface of bus 3 with an additional DER placed at the head of the feeder

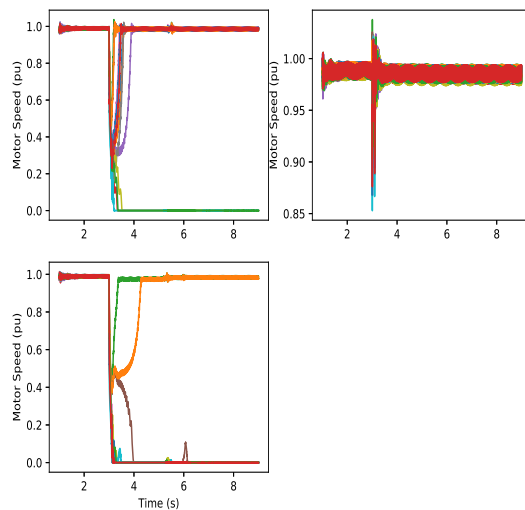


Figure 16: Speed of fourteen $1 - \phi$ induction motors on all three feeders (Feeder 3 top left, feeder 4 top right, feeder 18 bottom left) with an additional DER placed at the head of the feeder

4. Comparison of response with positive sequence models

Conventional power system planning utilizes positive sequence simulation methods and analysis. In this form of simulation, it is assumed that voltage and current across all three phases are balanced and thus only positive sequence quantities are used. Additionally, it is assumed that fast electromagnetic transients related to the transmission lines and cables are sufficiently damped and thus the network is represented using algebraic equations. Further, voltages and currents are represented as phasors about fundamental frequency. Further, in state of the art positive sequence studies, the dynamic behavior of loads and DER connected at the substation are represented using an aggregated model termed as a composite load model with distributed generation [14]. This aggregated model has: (i) electrical representations of aggregated behavior of $3 - \phi$ induction motors driving loads with different speed-torque characteristics, (ii) performance based model representing the aggregated behavior of $1 - \phi$ induction motors, (iii) representation of static and power electronic load, and (iv) representation of the aggregated behavior of power electronic based DERs using the DER_A model [2].

However with the proliferation of bulk power system connected inverter based resources and distribution system connected power electronic interfaced distributed energy resources there is a concern that conventional positive sequence simulation tools would not be able to completely capture all aspects of the dynamic behavior associated with these fast power electronic devices. While there certainly is technical justification behind this concern, and there is no doubt that positive sequence simulation environments would not be able to capture the dynamic behavior to a high degree of detail (especially at frequencies away from nominal frequency, during unbalanced network

Table 3: Summary of number of $1 - \phi$ induction motors that were able to successfully ride through the faults at buses 3, 4, and 18

Case	Fault Type	Load Pocket	Bus 3	Bus 4	Bus 18
0	LLL-G	Yes	1	11	1
	LL	Yes	8	11	8
	L-G	Yes	13	14	14
	L-G delayed	Yes	11	14	12
	LLL-G	No	3	10	3
	LL	No	9	12	9
	L-G	No	14	14	14
	L-G delayed	No	13	14	14
1	LLL-G	Yes	1	11	1
2	LLL-G	Yes	3	14	1
3	LLL-G	Yes	3	14	2
4	LLL-G	Yes	4	14	2
5	LLL-G	Yes	9	14	2
6	LLL-G	Yes	11	14	3
7	LLL-G	Yes	14	14	3
8	LLL-G	Yes	3	14	2
9	LLL-G	Yes	10	14	2
	LL	Yes	9	14	8
	L-G	Yes	14	14	14
	L-G delayed	Yes	14	14	13
	LLL-G	No	10	14	3
	LL	No	12	14	9
	L-G	No	14	14	14
	L-G delayed	No	14	14	14

conditions, and with regard to sub-cycle transient behavior), one has to also consider the practical challenges associated with electric utilities adopting simulation environments beyond positive sequence. Couple of crucial questions that should be asked that could aid in making a decision regarding this transition can be:

1. Is the behavior obtained from a positive sequence aggregated composite load model insufficient for transmission planners to make an informed decision about the impact of DER and load on the bulk power system?
2. If the behavior is sufficient, will it be sufficient even under future increased DER percentage levels?

In previous studies [38, 39], parameterization of the components of this aggregated model have been discussed. Here in this work, the dynamic behavior of the aggregated positive sequence model will be compared against the behavior observed in the detailed EMT simulations to ascertain the sufficiency of the aggregated model under a scenario of zero-inertia on bulk power system, high DER percentage in the distribution network, along with presence of FIDVR. Using the GE-PSLFTM positive sequence simulation software, the same modified transmission network is considered. The dynamic behavior of the bulk power system connected IBRs was represented using the REGC_C + REEC_A models along with an external auxiliary model to represent frequency droop control behavior. Load that was directly connected to the transmission system was represented using a static load model with constant current for active power and constant impedance for reactive power. The three feeders were represented using the *CMPLDWg* composite load with distributed generation model. The method of invoking the com-

posite load model with distributed energy resources in the dynamic data file of the positive sequence simulation software is provided in the Appendix. The description of each parameter can be found in [14, 40, 41] along with the appropriate block diagrams.

Within the composite load model, the static load model is used to represent the lighting load (LED based and incandescent) and resistive space heating and resistive oven loads. As such LED lighting is represented as constant current (which has been shown by multiple testing at EPRI and other research organizations and accepted by the industry) and the remaining loads are represented as constant resistance [14, 42, 43]. Note that the composite load model has motor components that represent the motor loads as well as a power electronic components (in addition to the static component) that covers all switch mode power supplies and converter type loads which have a constant power behavior over a wide voltage range.

It should be emphasized that the phasor model used here is an aggregated model, whereas the EMT model is a detailed model of individual load/equipment. This aggregated phasor model tries to capture the aggregated response of all the underlying individual models, that are distributed along the feeder. Therefore, the responses of the phasor model can be more, or less, conservative depending on the underlying system that is being aggregated as well as the fault that is being studied. Furthermore, the phasor model, which is an aggregated model, can always be tuned to match the aggregated response of the detailed load within an acceptable margin of error using any least squares algorithm. The authors would like to point out here that the aggregated models are used for typical transmission planning studies where thousands of instances of such models are used. Since these will vastly outnumber models of power plant and other transmission devices, it is an industry practice to make sure that the aggregated phasor model responses are neither too pessimistic nor too optimistic systemwide.

For the *_cmp_der_a* model (which is structurally the same as the DER_A model), the values of the parameters shown above are used as the default settings for all studied cases. However, depending on the particular DER scenario that was being analyzed (based upon the assumed operational mode of the DER listed in Table 2), the values of three parameters namely “*vl1*”, “*vl0*”, and “*kqv*” were appropriately changed. For *Case 1*, “*vl1*” = 0.90 and “*vl0*” = 0.85. For *Case 2*, *Case 4*, *Case 5*, and *Case 9*, “*vl1*” = 0.55 and “*vl0*” = 0.45. Finally, as the DER_A model is meant to represent the aggregated behavior of all DER on the feeder, for *Case 5*, “*kqv*” = 5.0 while for *Case 4* and *Case 9*, “*kqv*” = 2.50.

Although the values of the parameters of the *CMPLDWg* model did not change with change in DER scenario being studied, few of the parameters of the performance based model representing the aggregated behavior of $1 - \phi$ induction motors had to be different across the three buses (bus 3, bus 4, and bus 18) where the model was placed. At bus 3, “*Vrst*” = 0.80 and “*vtr1*” = 0.80. At bus 4, “*Vrst*” = 0.625 and “*vtr1*” = 0.60 while at bus 18, “*Vrst*” = 0.725 and “*vtr1*” = 0.60. A value of “*Tstall*” = -1.0 enables use of in-built stall curves in positive sequence software [40]. These curves have been derived from laboratory tests of air conditioners subjected to time varying voltage sags.

For the base case without any DER (denoted as Case 0 in Table 2), the comparison of the dynamic behavior between a full detailed EMT simulation and the aggregated behavior from a positive sequence model observed at buses 3, 4, and 18 is shown in Figs. 17-19 for an LLL-G fault with creation of a load pocket. It can be seen that the aggregated load model is able to provide a fair representation of the active and reactive power drawn by each of the three feeders while also providing a reasonable representation of the voltage magnitude both on the 230 kV side and the 12.47 kV side. However, due to differences in modeling of transmission lines between EMT domain and positive sequence domain, there is a bit of difference in the 230 kV voltage profile.

Upon adding DERs at buses 3 and 4, with a momentary cessation threshold of 0.88pu (denoted as Case 1 in Table 2), the comparison of the dynamic response observed at bus 3 and bus 4 is shown in Figs. 20 and 21. Here, due to the DERs going into momentary cessation, and with the load pocket depressing transmission level voltages following the clearance of the fault, the DERs and 1 – ϕ induction trip. In these scenarios too, the dynamic behavior from the positive sequence simulation shows the same trend as the response observed from the detailed EMT simulations. Because there were no DER added to bus 18, the dynamic behavior at bus 18 is not shown, but the response is very similar to that observed in Fig. 19.

With a lowering of the momentary cessation threshold to 0.50 pu (denoted as Case 2 in Table 2), comparison of the dynamic behavior at bus 3 and bus 4 is shown in Figs. 22 and 23. Here, although the response at bus 3 shows the same trend between positive sequence and EMT domain, the response observed at bus 4 shows a more conservative behavior in the positive sequence simulation model. In the detailed EMT simulation, at bus 4 with a reduction of DER momentary cessation threshold to 0.50 pu, all 1 – ϕ induction motors were able to successfully ride through the fault. The response from the positive sequence model shows a conservative behavior indicating that a higher number of 1 – ϕ induction motors may go into a stall condition and trip which is primarily

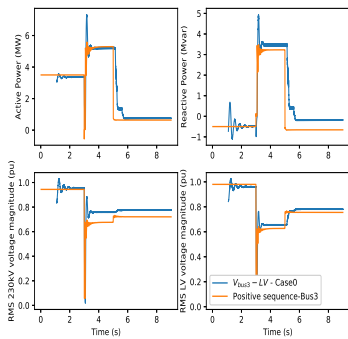


Figure 17: Without DERs, comparison of the system response at bus 3 between EMT and positive sequence for an LLL-G fault with creation of a load pocket

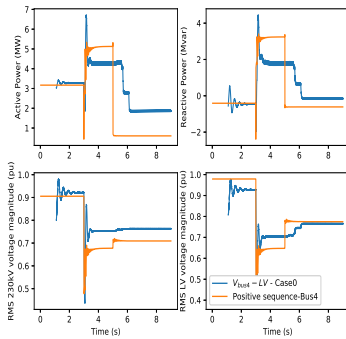


Figure 18: Without DERs, comparison of the system response at bus 4 between EMT and positive sequence for an LLL-G fault with creation of a load pocket

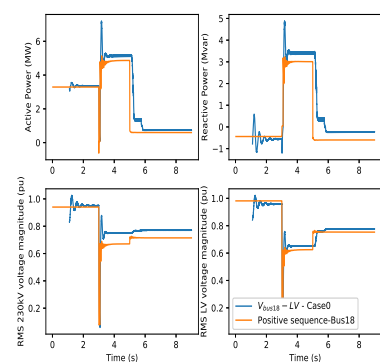


Figure 19: Without DERs, comparison of the system response at bus 18 between EMT and positive sequence for an LLL-G fault with creation of a load pocket

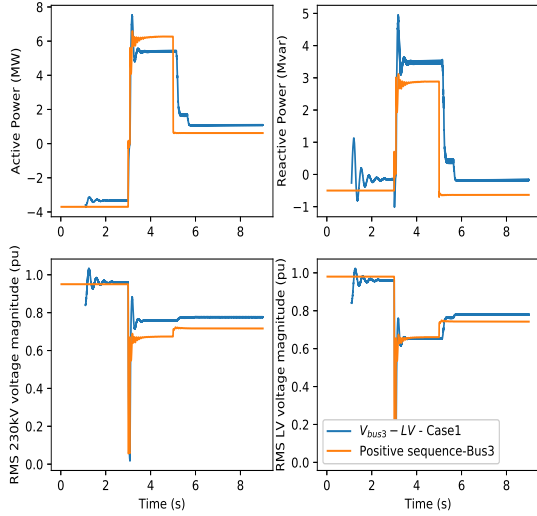


Figure 20: With DERs with a momentary cessation threshold of 0.88pu (Case 1 in Table 2), comparison of the system response at bus 3 between EMT and positive sequence for an LLL-G fault with creation of a load pocket

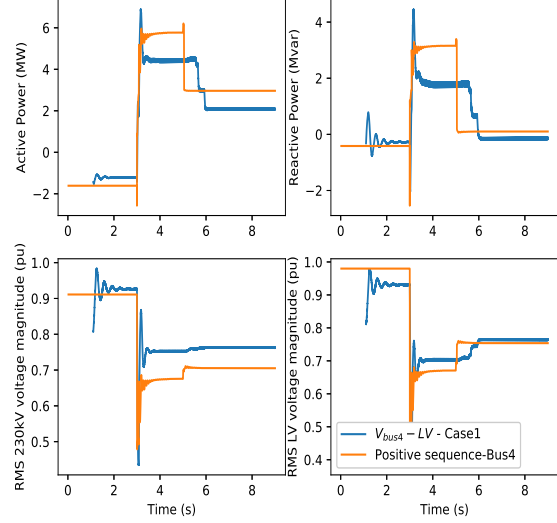


Figure 21: With DERs with a momentary cessation threshold of 0.88pu (Case 1 in Table 2), comparison of the system response at bus 4 between EMT and positive sequence for an LLL-G fault with creation of a load pocket

driven by the stall and restart voltage thresholds of the $1 - \phi$ induction motors in the performance based positive sequence model. However, although there is a difference in output, the trend of the response observed from the positive sequence model could possibly be sufficient to make informed transmission planning decisions.

With additional DER located at the feeder head, along with provision of dynamic voltage support from DER (denoted as Case 9 in Table 2), comparison of the dynamic response is shown in Figs. 24 and 25 for bus 3 and bus 4. It can be seen that although there is a good match between the responses, and the performance observed aligns with recent work done to parameterize this model against measured data [44], there is still further work that can be done to improve either the aggregated model or the derivation of its parameter values. The parameters that play a crucial role in the response of the performance based model of $1 - \phi$ induction motors re-accelerates to a steady state running condition (V_{rst}) and the upper value of the under voltage trip threshold (v_{tr1}). In the detailed EMT model, the trip of the $1 - \phi$ induction motors occurs based on its measured speed. However, since the performance model in the composite load model does not have this attribute, tripping of the motors is initiated using the under voltage trip settings. While the values for voltage threshold can be parameterized adequately, further research work is to be carried out in order to obtain an analytical method of calculating the settings. Also, this work also points towards the need for improvement of single phase induction motor models both in EMT domain and positive sequence domain.

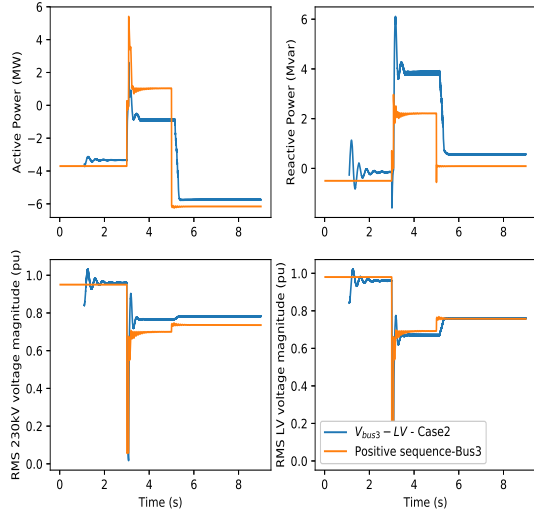


Figure 22: With DERs with a momentary cessation threshold of 0.50pu (Case 2 in Table 2), comparison of the system response at bus 3 between EMT and positive sequence for an LLL-G fault with creation of a load pocket

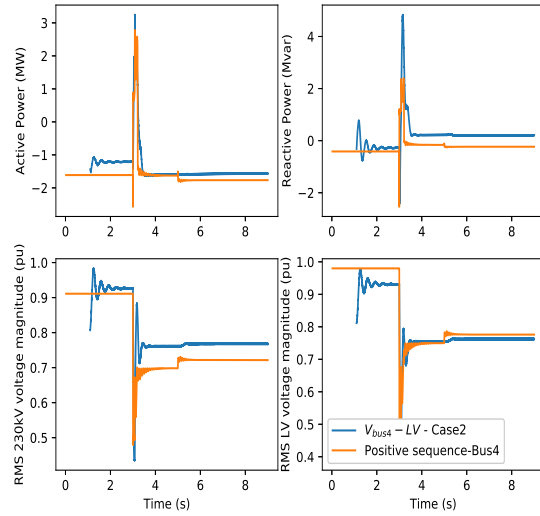


Figure 23: With DERs with a momentary cessation threshold of 0.50pu (Case 2 in Table 2), comparison of the system response at bus 4 between EMT and positive sequence for an LLL-G fault with creation of a load pocket

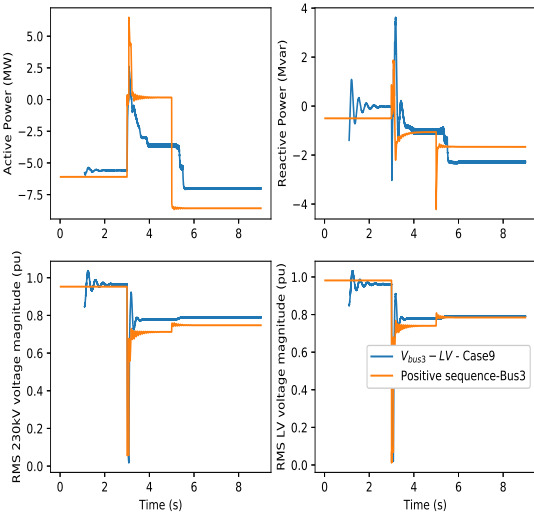


Figure 24: With DERs providing dynamic voltage support (Case 9 in Table 2), comparison of the system response at bus 3 between EMT and positive sequence for an LLL-G fault with creation of a load pocket

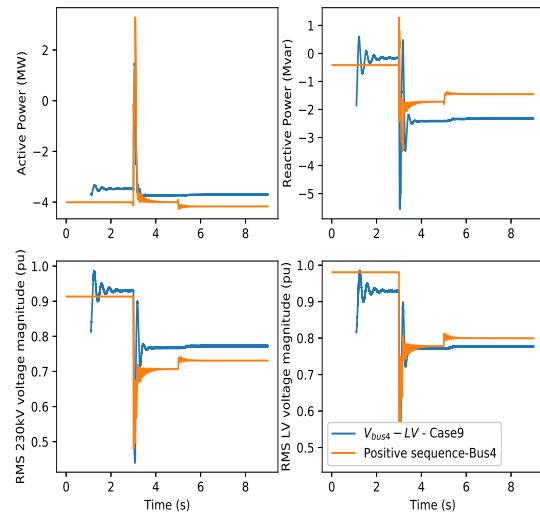


Figure 25: With DERs providing dynamic voltage support (Case 9 in Table 2), comparison of the system response at bus 4 between EMT and positive sequence for an LLL-G fault with creation of a load pocket

5. Conclusion

In this paper, a detailed analysis is carried out to ascertain the potential benefit of dynamic voltage support from DERs, especially with regard to the stalling and re-acceleration of 1 – ϕ induction motors. Dynamic voltage support from 3 – ϕ DERs

connected at 12.47kV locations along a reduced distribution feeder has been shown to improve the fault ride through behavior of the induction motors. Further, the ability of the state of the art positive sequence composite load model to represent the behavior observed in detailed EMT simulation has also been illustrated. Although there exists a difference in the absolute value of active and reactive power, the trend of the response is the same across both simulation platforms. There are few reasons for the difference in the absolute values with transformer saturation and line charging representation being different across the two platforms. Here, since the trend of the response is the same across the two platforms, the impact on the bulk power system is the same, irrespective of the actual absolute value of the powers. A transmission planner who may use the phasor model can arrive at the same conclusions regarding the system behavior when using either model and as a result, we conclude that the trend of the response is the same from the perspective of the planner. Future work includes extending the analysis to include single phase DERs in the electromagnetic analysis to observe any potential impact of dynamic voltage support.

References

- [1] “IEEE Standard for Interconnecting Distributed Resources with Electric Power Systems,” *IEEE Std 1547-2003*, pp. 1–28, 2003.
- [2] I. Alvarez-Fernandez et al., “Impact analysis of ders on bulk power system stability through the parameterization of aggregated der_a model for real feeders,” *Electric Power Systems Research*, vol. 189, no. 106822, 2020.
- [3] M. H. J. Bollen, *Understanding Power Quality Problems*. Wiley-IEEE Press, 2000.
- [4] Myo Thu Aung and J. V. Milanovic, “The influence of transformer winding connections on the propagation of voltage sags,” *IEEE Transactions on Power Delivery*, vol. 21, no. 1, pp. 262–269, 2006.
- [5] N. Hatziaergyriou, J. V. Milanovic, C. Rahmann, V. Ajjarapu, C. Canizares, I. Erlich, D. Hill, I. Hiskens, I. Kamwa, B. Pal, P. Pourbeik, J. J. Sanchez-Gasca, A. M. Stankovic, T. Van Cutsem, V. Vittal, and C. Vournas, “Definition and classification of power system stability revisited extended,” *IEEE Transactions on Power Systems*, pp. 1–1, 2020.
- [6] “IEEE Standard for Interconnecting Distributed Resources with Electric Power Systems - Amendment 1,” *IEEE Std 1547a-2014 (Amendment to IEEE Std 1547-2003)*, pp. 1–16, 2014.
- [7] “IEEE Standard for Interconnection and Interoperability of Distributed Energy Resources with Associated Electric Power Systems Interfaces,” *IEEE Std 1547-2018 (Revision of IEEE Std 1547-2003)*, pp. 1–138, 2018.

- [8] “IEEE Standard for Interconnection and Interoperability of Distributed Energy Resources with Associated Electric Power Systems Interfaces—Amendment 1: To Provide More Flexibility for Adoption of Abnormal Operating Performance Category III,” *IEEE Std 1547a-2020 (Amendment to IEEE Std 1547-2018)*, pp. 1–16, 2020.
- [9] “Transmission and Distribution Operations and Planning Coordination: TSO/DSO and Tx/Dx Planning Interaction, Processes, and Data Exchange,” EPRI, Palo Alto, CA., Tech. Rep. 3002016712, 2019.
- [10] “A Technical Reference Paper Fault-Induced Delayed Voltage Recovery,” North American Electric Reliability Corporation, Tech. Rep., 2009.
- [11] J. W. Shaffer, “Air conditioner response to transmission faults,” *IEEE Transactions on Power Systems*, vol. 12, no. 2, pp. 614–621, 1997.
- [12] B. R. Williams, W. R. Schmus, and D. C. Dawson, “Transmission voltage recovery delayed by stalled air conditioner compressors,” *IEEE Transactions on Power Systems*, vol. 7, no. 3, pp. 1173–1181, 1992.
- [13] L. Y. Taylor and Shih-Min Hsu, “Transmission voltage recovery following a fault event in the metro atlanta area,” in *2000 Power Engineering Society Summer Meeting (Cat. No.00CH37134)*, vol. 1, 2000, pp. 537–542 vol. 1.
- [14] NERC Load Modeling Task Force (LMTF), “Technical Reference Document: Dynamic Load Modeling,” NERC, Atlanta, GA., Tech. Rep., December 2016.
- [15] B. Lesieutre, R. Bravo, R. Yinger, D. Chassin, H. Huang, N. Lu, I. Hiskens, and G. Venkataramanan, “Final Project Report – Load Modeling Transmission Research,” Lawrence Berkeley National Laboratory (LBNL), Tech. Rep., 2010.
- [16] M. Paramasivam, A. Salloum, V. Ajjarapu, V. Vittal, N. B. Bhatt, and S. Liu, “Dynamic optimization based reactive power planning to mitigate slow voltage recovery and short term voltage instability,” *IEEE Transactions on Power Systems*, vol. 28, no. 4, pp. 3865–3873, 2013.
- [17] A. Tiwari and V. Ajjarapu, “Addressing short term voltage stability problem - part i: Challenges and plausible solution directions,” in *2016 IEEE/PES Transmission and Distribution Conference and Exposition (T D)*, 2016, pp. 1–5.
- [18] —, “Addressing short term voltage stability problem - part ii: A case study,” in *2016 IEEE/PES Transmission and Distribution Conference and Exposition (T D)*, 2016, pp. 1–5.
- [19] A. H. Al-Mubarak, S. M. Bamsak, B. Thorvaldsson, M. Halonen, and R. Grunbaum, “Preventing voltage collapse by large svcs at power system faults,” in *2009 IEEE/PES Power Systems Conference and Exposition*, 2009, pp. 1–9.

- [20] G. Reed, B. Grainger, M. Kempker, P. Bierer, A. Such, R. Grubb, D. Sullivan, D. Shoup, B. Buterbaugh, and J. Paramalingam, “Technical requirements and design of the indianapolis power and light 138 kv southwest static var compensator,” in *2016 IEEE/PES Transmission and Distribution Conference and Exposition (TD)*, 2016, pp. 1–5.
- [21] D. Sullivan, R. Pape, J. Birsa, M. Riggle, M. Takeda, H. Teramoto, Y. Kono, K. Temma, S. Yasuda, K. Wofford, P. Attaway, and J. Lawson, “Managing fault-induced delayed voltage recovery in metro atlanta with the barrow county svc,” in *2009 IEEE/PES Power Systems Conference and Exposition*, 2009, pp. 1–6.
- [22] A. Boström, R. Grunbaum, M. Dahlblom, and H. V. Oheim, “Svc for reliability improvement in the nstar 115 kv cape cod transmission system,” in *2013 IEEE Power Energy Society General Meeting*, 2013, pp. 1–5.
- [23] “Common Functions for Smart Inverters 4th Edition,” EPRI, Palo Alto, CA., Tech. Rep. 3002008217, 2016.
- [24] R. J. Bravo, “Der volt-var and voltage ride-through needs to contain the spread of fidvr events,” in *2015 IEEE Power Energy Society General Meeting*, 2015, pp. 1–3.
- [25] R. K. Varma and S. Mohan, “Mitigation of fault induced delayed voltage recovery (fidvr) by pv-statcom,” *IEEE Transactions on Power Systems*, vol. 35, no. 6, pp. 4251–4262, 2020.
- [26] B. Park and M. M. Olama, “Mitigation of motor stalling and fidvr via energy storage systems with signal temporal logic,” *IEEE Transactions on Power Systems*, vol. 36, no. 2, pp. 1164–1174, 2021.
- [27] W. Wang and F. de León, “Quantitative evaluation of der smart inverters for the mitigation of fidvr in distribution systems,” *IEEE Transactions on Power Delivery*, vol. 35, no. 1, pp. 420–429, 2020.
- [28] “An Overview of Co-Simulation Platforms for Transmission Planning,” EPRI, Palo Alto, CA., Tech. Rep. 3002017494, 2019.
- [29] M. A. Pai, *Energy function analysis for power system stability*. Kluwer Academic Publishers, 1989.
- [30] P. Mitra, A. Gaikwad, and J. C. Boemer, “Impact of Distributed Energy Resources (DER) Voltage Regulation and Ride-Through Settings on Distribution Feeder Voltage Recovery,” in *CIGRÉ U.S. National Committee, Grid of the Future Symposium*, Cleveland, OH, Oct. 2017.

- [31] “Impact of DER Voltage Regulation and Voltage Ride-Through Settings on Fault-Induced Delayed Voltage Recovery (FIDVR),” EPRI, Palo Alto, CA., Tech. Rep. 3002009363, 2017.
- [32] “Impact of DER Voltage Regulation and Voltage Ride-Through Settings on Fault-Induced Delayed Voltage Recovery,” EPRI, Palo Alto, CA., Tech. Rep. 3002011112, 2017.
- [33] D. Ramasubramanian, W. Baker, and E. Farantatos, “Operation of an all inverter bulk power system with conventional grid following controls,” *CIGRÉ Science & Engineering*, vol. 18, pp. 62–76, 2020.
- [34] Y. Liu, V. Vittal, J. Undrill, and J. H. Eto, “Transient model of air-conditioner compressor single phase induction motor,” *IEEE Transactions on Power Systems*, vol. 28, no. 4, pp. 4528–4536, 2013.
- [35] Y. Liu, “Modeling of air-conditioner compressor single phase induction motor for transient analysis,” Master’s thesis, Arizona State University, 2012.
- [36] L. Sundaresh, P. Mitra, D. Ramasubramanian, A. Gaikwad, and E. Farantatos, “Impact of large scale integration of inverter-based resources on fidvr,” in *2020 North American Power Symposium*, 2020, pp. 1–6.
- [37] “IBR Modeling Guidelines for Weak Grid Studies and Case Studies,” EPRI, Palo Alto, CA., Tech. Rep. 3002018719, 2020.
- [38] “Detailed Distribution Circuit Analysis and Parameterization of the Partial Voltage Trip Logic in WECC’s DER Model (DER_A): Improvements for Modern and Single Phase DER and Regional Default Settings for Unbalanced Fault Conditions,” EPRI, Palo Alto, CA., Tech. Rep. 3002016685, 2019.
- [39] “Technical Update on Load Modeling,” EPRI, Palo Alto, CA., Tech. Rep. 3002016290, 2019.
- [40] General Electric International, Inc, “Positive Sequence Load Flow (PSLF),” Tech. Rep., 2020.
- [41] “Technical Reference on the Composite Load Model,” EPRI, Palo Alto, CA., Tech. Rep. 3002019209, 2020.
- [42] P. Kundur, *Power System Stability and Control*. McGraw-Hill Education, 1994.
- [43] A. Bokhari, A. Alkan, R. Dogan, M. Diaz-Aguiló, F. de León, D. Czarkowski, Z. Zabar, L. Birenbaum, A. Noel, and R. E. Usef, “Experimental determination of the zip coefficients for modern residential, commercial, and industrial loads,” *IEEE Transactions on Power Delivery*, vol. 29, no. 3, pp. 1372–1381, 2014.

- [44] P. Pourbeik, D. J. Ryan, F. Brnadic, J. Riesz, B. Badrzadeh, and J. Lu, “Developing dynamic load models for the australian national electricity market with a focus on distributed energy resources,” *CIGRÉ Science & Engineering*, vol. 20, pp. 91–105, 2021.

6. Appendix

```

_cmp_der_a -110 : /
"trv" 0.02 "dbd1" -0.1 "dbd2" 0.1 "kqv" 0.0 "vref0" 0.0 "tp" 0.02 /
"pfflag" 1 "tiq" 0.02 "ddn" 20.0 "dup" 20.0 "fdbd1" 0.000283 "fdbd2" /
0.000283 "femax" 99 "femin" -99 "pmax" 1.1 "pmin" 0 "frqflg" 0 /
"dPmax" 0.5 "dPmin" -0.5 "tpord" 0.02 "imax" 1.0 "pqflag" 0 "v10" 0.85 /
"v11" 0.9 "vh0" 1.25 "vh1" 1.15 "tv10" 0.16 "tv11" 0.16 "tvh0" 0.16 /
"tvh1" 0.16 "vrfrac" 1.0 "fltrp" 59.0 "fhtrp" 61.0 "tfl" 5.0 "tfh" 5.0 /
"tg" 0.02 "rrpwr" 10.5 "tv" 0.02 "kpg" 0.1 "kig" 10.0 "xe" 0.2 /
"typeflag" 1 "vfth" 0.8 "iqh1" 1.0 "iql1" -1.0

cmpldwg busno "Bus Name" basekV "ID" : #9 mva=-0.58 "bss" 0.00586 "rfdR" 0.04 /
"xfdr" 0.04 "fb" 1.0000 "xxf" 0.09983 "tfixhs" 1.0000 "tfixls" 1.0200 /
"ltc" 1.0000 "tmin" 0.9000 "tmax" 1.1000 "step" 0.006250 "vmin" 0.950 "vmax" 1.0125 /
"tdel" 30.0000 "ttap" 5.0000 "rcmp" 0.0000 "xcmp" 0.0000 "fma" 0.0297 "fmb" 0.0001 /
"fmc" 0.0001 "fmd" 0.7211 "fel" 0.0001 "pfel" 1.0000 "vd1" 0.6500 "vd2" 0.5000 /
"frcel" 0.8000 "pfs" -0.990000 "p1e" 2.0 "p1c" 1.000000 "p2e" 1.0000 "p2c" 0.000000 /
"pfrq" 0.0000 "q1e" 2.0000 "q1c" 1.000000 "q2e" 1.0000 "q2c" 0.000000 "qfrq" 0.0000 /
"mtypa" 3.0 "mtypb" 3.0 "mtypc" 3.0 "mtypd" 1.0 "lfma" 0.8500 "Rs" 0.0400 /
"Rs" 1.8000 "Lp" 0.1200 "Lpp" 0.1040 "Tpo" 0.09500 "Tppo" 0.0021 "H" 0.1000 /
"etrq" 0.0000 "vtr1" 0.6500 "ttr1" 99.10 "ftr1" 0.2000 "vrc1" 99.6900 "trc1" 999.0 /
"vtr2" 0.0000 "ttr2" 99.020 "ftr2" 0.750 "vrc2" 99.6500 "trc2" 0.1000 "LFmb" 0.7500 /
"Rs" 0.0300 "Ls" 1.8000 "Lp" 0.19000 "Lpp" 0.1400 "Tpo" 0.200 "Tppo" 0.0026 /
"H" 0.5000 "etrq" 2.0000 "vtr1" 0.5500 "ttr1" 0.0200 "ftr1" 0.3000 "vrc1" 0.6500 /
"trc1" 0.05000 "vtr2" 0.5000 "ttr2" 0.0250 "ftr2" 0.3000 "vrc2" 0.6000 "trc2" 0.05000 /
"LFmc" 0.7500 "Rs" 0.03000 "Ls" 1.8000 "Lp" 0.18000 "Lpp" 0.14000 "Tpo" 0.2000 /
"Tppo" 0.00260 "H" 0.1000 "etrq" 2.0000 "vtr1" 0.5800 "ttr1" 0.03000 "ftr1" 0.20 /
"vrc1" 0.68000 "trc1" 0.0500 "vtr2" 0.53 "ttr2" 0.0300 "ftr2" 0.3000 "vrc2" 0.620 /
"trc2" 0.05 "LFmd" 1.0 "CompPF" 0.98000 "Vstall" 0.6 "Rstall" 0.15 "Xstall" 0.06 /
"Tstall" -1.0 "Frst" 1.0 "Vrst" 0.8 "Trst" 0.04 "fuvr" 1.0 "vtr1" 0.8000 /
"ttr1" 2.000 "vtr2" 0.20 "ttr2" 0.20 "Vc1off" 0.06 "Vc2off" 0.04 "Vc1on" 0.5 /
"Vc2on" 0.65 "Tth" 15.0 "Th1t" 0.70 "Th2t" 1.9000 "Tv" 0.025000 /
"DGtype" 2.0 "DGdatno" -110 "DGmbase" -0.8

```